SSRG International Journal of Mechanical Engineering
ISSN: 2348-8360/ https://doi.org/10.14445/23488360/IJME-V11I10P102

Volume 11 Issue 10, 8-25, October 2024

Original Article

Performance Evaluation of Al-ZrB_2 Reinforcement Based Metal Matrix Nanocomposites

Seema V. Yerigeri[1], Vaijanath V. Yerigeri[2]

[1]*Mechanical Engineering Department, M. B. E. Society's College of Engineering, Maharashtra, India.*
[2]*Electronics & Computer Engineering Department, M. B. E. Society's College of Engineering, Maharashtra, India*.

[1]*Corresponding Author : seemayerigeri1877@gmail.com*

Received: 02 August 2024 Revised: 03 September 2024 Accepted: 03 October 2024 Published: 30 October 2024

Abstract *- Lightweight and high-strength composites attract attention towards the different industrial applications. Reinforcement in base material makes composite operate at high working temperatures. In the present research, different Al based MMNC's are fabricated, friction and wear analysis using pin-on-disc is performed as tribological properties play a crucial role in deciding its performance. Many engineering components fail because of wear loss, which changes dimensions and fits between the mating components. Due to the poor tribological properties of aluminium alloys, their application in machine parts is limited. Incorporating small wt.% of nanoparticles enhances the wear rate and coefficient of friction. Enhancement of these tribological properties depends on factors like alloy grade, reinforcement type and its wt.%, load applied, and sliding distance. Al7075, Al6082, and Al6063 are selected as alloy levels, while ZrB_2 reinforcement levels are set at 6, 9, and 12 wt.%. Load and speed levels are set at 30N, 40N, 50N and 140, 150, 160 rpm. From Taguchi statistical analysis, an optimum combination of Al7075 with 12% ZrB_2 load at 30N gives, a minimum wear rate at the speed of 140 rpm and minimum COF at the speed of 160 rpm. The heat treatment effect on hardness and worn surface analysis of nanocomposites are also provided in the article.*

Keywords *- Composite materials, Taguchi, Pin-on disc, ZrB_2, ANOVA, Energy Dispersive X-ray Spectroscopy EDX, Scanning Electron Microscopy SEM.*

1. Introduction

Lightweight design is a concept in engineering where structures, machine parts, and products are crafted in a way to reduce weight substantially within the constraints. The primary goal of constructing this lightweight material is to retain or even extend the functionality of a product while the total weight of the product goes down. Current techniques that are used to reduce mass include using materials that are less dense, like composite materials and metal foams. Another way is to lower the volume of the material by thinning out the walls in the most important structural components. In both cases, the energy that is required to transport the ready products is far less and, in doing so, the pro-ecological aspect of lightweight construction is upheld. The concept guides us to utilize low-density material or lesser material without compromising the performance [1]. The result of lightweight design is the same component with the same or enhanced performance but with less mass. In the case of the transportation industry, this reduction in mass reduces the energy requirement to propel the vehicle, thus increasing the cruising range and efficiency [2]. A 100 kg reduction in vehicle weight will lead to a fuel saving of 0.3-0.5 l/km. A similar study shows 10-12 % of fuel efficiency with a reduction of 20 % in weight of Boing 787 [3]. Although parameters like friction losses, aerodynamic drag, etc., can be controlled to increase fuel efficiency, weight reduction is an easier method [3].

The International Civil Organization has set a target to reduce aviation emissions by fifty percent by the year 2050. New stricter restrictions imposed on different types of harmful emissions have forced automobile and aerospace industries to think about using lightweight materials for different machine components [4]. Aluminium is the most used engineering material after steel due to its higher strength-to-weight ratio than steel. Aluminium also has good ductility and formability; as a result, fabrication processes consume less energy.

Different properties other than pure metal can also be obtained by changing the alloying composition and heat treatment processes [4]. Aluminium is also one of the amplest metals on earth and makes up about eight percent of the earth's crust. Also, its recycling process consumes less energy. Considering all the above characteristics and properties, it can be concluded that aluminium is one of the ideally suited materials that can be used in lightweight applications.

Due to the above-mentioned properties of aluminium and its alloys, it is widely used in structural components in various fields which include transport, construction, and packaging. But use of aluminium in machine components that are subjected to relative motion or surface-to-surface contact is limited due to its inferior wear properties [5]. When methods like alloying, heat treatment and grain modification failed to provide the desired wear properties, researchers turned their exploration toward developing aluminium composites. Conventional micro-composites have shown better wear resistance, but other properties like ductility and formability have been reduced significantly. A recently developed category of material called nanocomposites is known to provide desired wear properties without significant or no loss in ductility.

Various researchers have reported the enhancement of tribological properties due to the addition of nanoparticles in aluminium alloys. Ali et al. [6] have studied the effect of the addition of tungsten nanoparticles in Al 6063 alloy on wear properties for probable application in engine block liners. The composite was fabricated by using the Friction Stir Processing (FSP) method. The results observed were a decrease in wear rate as the reinforcement content increased from 0 to 12 %, coefficient of friction was also reduced due to the presence of tungsten nanoparticles. Along with this wear property increment in hardness and grain refinement is also observed. Ramchandra et al. [7] fabricated Al-ZrO_2 nanocomposite by powder metallurgy process. From the test result, the observation was that the wear rate decreases with the increase in ZrO_2 nanoparticles in the aluminium matrix. Oxidation, thermal softening, and micro-cutting are reported as the predominant wear mechanisms. Samal et al. [8] studied the wear behaviour of Al 6082 composite reinforced with red mud particles. The composite was fabricated by the stir casting method with Al 6082 billets and red mud particles with 500-50nm size. The wear test was performed on the pin-on-disk machine, which showed a decrease in wear rate as red mud particles increased from 0 to 6%. A lower coefficient of friction was observed for higher reinforcement content. Abrasion and delamination were reported as the dominant wear mechanisms from the analysis of SEM micrographs. Al-Salihi et al. studied the effect of Al_2O_3 nanoparticles on AA7075 alloy. The composite was fabricated by the stir casting method. The test results have shown a 14.3% improvement in Ultimate Tensile Strength (UTS) and a 34.3% improvement in Yield Tensile Strength (YTS) for 5% Al_2O_3 reinforcement. This increase is mainly due to the restrictions offered by Al_2O_3 particles to the dislocation movement. A wear test was also conducted on the pin-on-disk machine, which showed a decrease in the wear rate with an increase in reinforcement content.

The hardness of the 5% Al_2O_3 composite is also increased by 26.3% [9]. In a similar study, Al 7075 alloy reinforced with micron size B_4C reinforcement showed a decrease in wear rate as the weight fraction of reinforcement increased from 6 to 8%. The composite was fabricated by the stir casting method with the varying weight fraction of reinforcement. Later, it was subjected to solution treatment and age hardening. The comparison between Age-hardened and As-cast composites shows a lower wear rate for age-hardened composites [10]. One of the lightest metals used for structural applications is aluminium. It has a density of 2.7gm/$cm^{3,}$ which is about a third of steel. It is available very easily and, due to its weight, is very popular in applications that must be weight efficient like space, aerospace, sports, automotive and electronic industries. The beneficial properties of aluminium, such as high ductility, strong resistance to corrosion and advantageous strength/weight ratio, also make it very attractive. Based on the needed application, it is possible to use both, the micro as well as the nano length scale particles as reinforcers in the metal matrix. However, nanoparticles have been used increasingly in the composites as reinforcers thereby replacing other kinds of reinforcers like nano-whiskers, nanoplatelets or nanofibers because they are easy to manufacture at lower costs. The most extensively utilized types of nanoparticles are TiC, B_4C, SiC, Si_3N_4, AlN, SiO_2, Al_2O_3, graphene nanoparticles, and some others. Figure 1 illustrates applications in which aluminium matrix nanocomposites are being used. However, the disadvantage of using traditionally processed material is that the particles are not homogenously dispersed, and there is low interfacial integrity between the aluminium matrix and the reinforcement particles. However, further studies and research are ongoing in the evolution of compositional alterations of nanocomposites and the techniques to make them. The aim of such studies is to eliminate the drawbacks and also to attain enhanced microstructural properties.

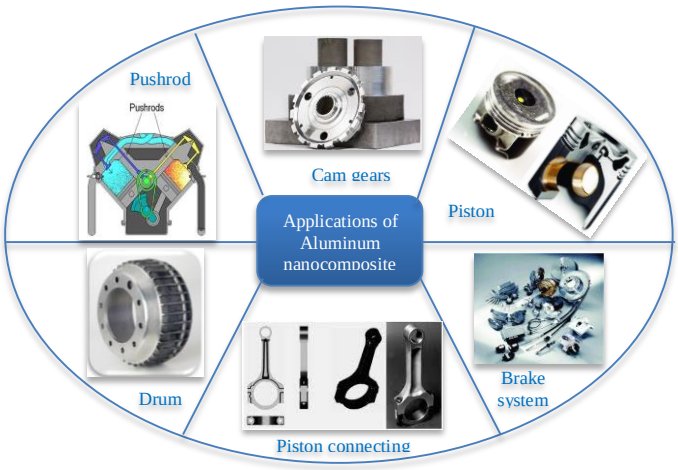

Fig. 1 Uses of Al nanocomposites in various mechanical components

From the above literature, it can be concluded that the upcoming generations of automobiles and other industrial components will necessitate improved tribological attributes in tandem with a reduction in weight. To that end, it will be crucial that the existing materials, such as steel, be replaced

with lightweight materials, such as aluminium metal matrix composites that have been reinforced with particles of ceramic. Aluminium MMNCs are the low-cost answer to the traditional materials used in tribological applications. Tribological properties are enhanced due to the addition of reinforcement particles of nanosized in the base metal. Since most of the authors have studied the wear behavior of single-base aluminium alloy, comparison between these alloys for tribological properties sometimes becomes a difficult task. To overcome the issues mentioned above, this research work compares the performance of different aluminium alloys along with the other parameters, including reinforcing content, load, and speed, which provide minimum wear rate and friction. Figure 2 shows a schematic representation of the adopted process. The process consists of the fabrication of the nanocomposite by selecting different aluminium alloys and a suitable reinforcement. After comparing different fabrication processes, the stir casting method is selected to manufacture the billets of nanocomposites. These billets of nanocomposites are then machined on a CNC lathe to obtain the desired dimension of the samples. These machined samples are then heat-treated. To observe the effect of the heat treatment process, hardness data was recorded before and after the process. The heat-treated samples are then tested on a pin-on-disc machine to obtain the friction and wear data. This data is then analysed to obtain the optimum combination of the above-mentioned parameters. Material characterization techniques like SEM and EDX are applied to obtain the wear mechanisms, nanoparticle distribution in the matrix and worn surface composition.

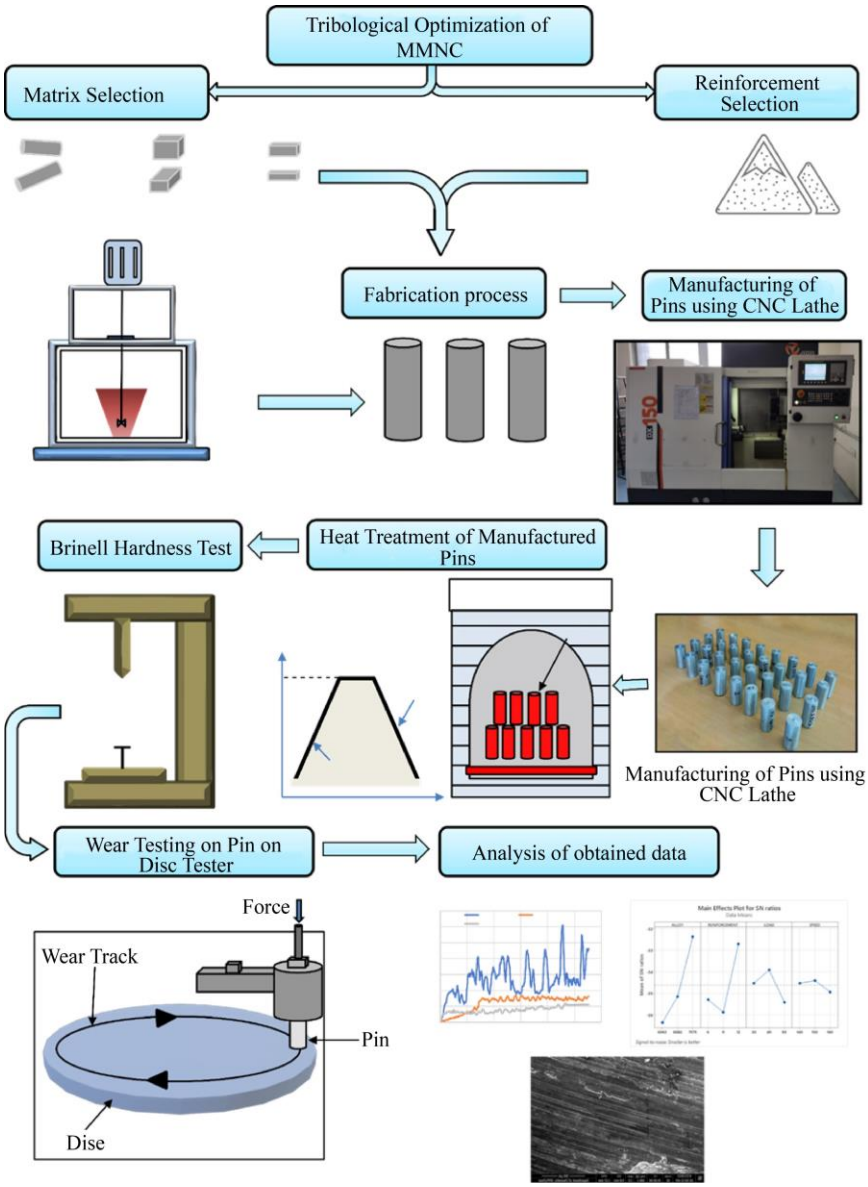

Fig. 2 Schematic representation of adapted process

2. Materials And Methodology

2.1. Materials

2.1.1. Base Materials

Aluminium is the most popular engineering material for the aerospace industry. It contributes to approximately 60-80% of airframe weight in modern space vehicles, helicopters, and aircraft. Pure aluminium has a lower density (2.7 g/cm^3) in contrast to steel (7.9 g/cm^3), which helps to reduce the weight of machine components and the fuel requirement to propel the vehicle or an aircraft [11, 12]. Aluminium has high ductility; hence it can be formed into different machine parts easily. Due to its low melting point and high ductility, the energy required for the fabrication process is less as compared to steel. Aluminium has high thermal conductivity due to which it is also most widely used to manufacture heat exchangers and cooking appliances along with other machine parts in automobile and aerospace industries. In corrosive environments, aluminium forms a protective oxide layer that safeguards the material from the adverse effects of corrosion.

Different aluminium alloy grades enhance different properties, and hence, they have different applications. Al 6063 is most widely used in automotive parts, architectural extrusion, and other machine parts. Al 7075 is used in high-strength aircraft parts, while Al 6082 is used in cranes, trusses, and cargo containers. Hence, Al-6063, Al-6082 and Al-7075 were selected for the nanocomposite fabrication due to the above-mentioned application areas. The composition of the selected aluminium alloys is summarized in Table 1 [13, 14].

Table 1. The composition and application of Al 6063, Al 6082, and Al 7075 alloys

Al Alloy	Composition (%)								
	Si	Fe	Cu	Mn	Mg	Cr	Zn	Ti	Al
6063	0.60	0.35	0.10	0.10	0.9	0.10	0.10	0.10	97.65
6082	1.30	0.50	0.10	1.00	1.2	0.25	0.20	0.10	95.35
7075	0.40	0.50	2.00	0.30	2.9	0.28	6.10	0.20	87.32

Table 2. Properties of zirconium diboride ZrB_2

Properties of Zirconium-Di-Boride (ZrB_2)	
Crystall System Space Group	Hexagonal
Melting Point (°C)	3245
Density (g /cm^3)	6.119
Young's Modulus (GPa)	489
Hardness (GPa)	23
Coefficient of Thermal Expansion (K^{-1})	5.9x10^{-6}
Thermal Conductivity (W/m K)	60
Bulk Modulus (GPa)	215
Heat Capacity (J/(mol.K)$^{-1}$)	48.2

2.1.2. Reinforcement Material

Zirconium Di-Boride (ZrB_2) is one of the ultra-high temperature ceramic materials that has a melting temperature exceeding 3000°c. The ZrB_2 particle has high chemical stability, high thermal and electrical conductivity, and high resistance to corrosion. It has a hexagonal crystal structure. The brittleness and hardness of ZrB_2 particles are lower than carbides. These properties of ZrB_2 also remain stable even at high temperatures. The properties of ZrB_2 particles are listed in Table 2 [15].

2.2. Experimental Methodology

2.2.1 Fabrication of Nanocomposites by Stir Casting Method

Nanocomposites can be fabricated by different processing methods, which include solid-state processing, semisolid-state processing, liquid-state processing, and gaseous-state processing. Among the different methods of processing, liquid state processing is most frequently selected to fabricate aluminium nanocomposites due to the flexibility of the process and the low cost of fabrication [16].

Stir casting is the most widely used cost-effective method of nanocomposite fabrication, also called vortex casting. In this method, a stirrer rotating at high speed draws and distributes the nanoparticles in the molten matrix [17-19].

The schematic layout of the stir casting setup used to fabricate nanocomposites is shown in Figure 3(a) and casted billets are shown in the Figure 3(b).

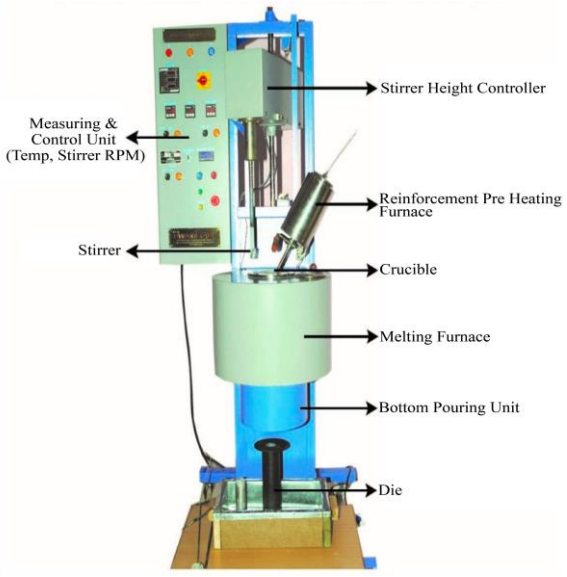

Fig. 3 (a) Stir casting setup

Machine Specifications

1. Machine Name: Bottom Pouring Stir Casting Furnace
2. Make: SWAMEQUIP
3. Model: AI
4. A.C. supply: 230 V
5. Stirrer Speed range:100 – 1500 rpm

It consists of an electronically controlled mechanical stirrer, a melting furnace, a reinforcement preheating furnace and a reinforcement feeder. The base metal is heated to a molten state in a melting furnace. A preheating furnace also heats the reinforcement material to a specific temperature to remove moisture and boost the wettability of the reinforcement material. Then the preheated reinforcement powder is added to the molten metal by using a feeder. This mixture of molten metal and reinforcement particles is stirred by operating the stirrer. To avoid the settling of the nanoparticles at the bottom of the mould, a bottom-taping technique was adapted. To achieve uniform distribution of nanoparticles, a two-step filler feeding method is used in which half the volume of the mould is first filled with molten alloy, and the corresponding weight fraction of reinforcement is added. After mixing with the stirrer, the remaining part of the mould is filled with reinforcement and base metal and then the whole mixture is stirred by using a stirrer. After sufficient stirring, the molten nanocomposite is allowed to cool slowly in a preheated die.

Observations during Fabrication

1. ZrB_2 sparkles when it reacts with the air (Like Magnesium).
2. A huge density difference was seen between ZrB_2 and the matrix with less wettability.
3. With the maximum temperature of about 800°C plus, ZrB_2 completely turns like ash.
4. So, the ZrB_2 was preheated up to 400°C.
5. The mould was preheated up to 250°C
6. Two-step feeding method was adopted.
7. The set-up was completely fixed under vacuum, even though when pouring in the mould sparkle of ZrB_2 occurred.

Fig. 3 (b) Stir casted Al MMNC billets (Al-6063, Al-6082, Al-7075) with 6%, 9% and 12% ZrB_2

2.2.2. Machining of Casted Billets on CNC Lathe

To obtain wear and friction data pin-on-disk apparatus was used. Cylindrical samples (Figure 3 (c)) of 10mm diameter and 25mm length were prepared with a CNC lathe as per the standard test method (ASTM G 99-95a) for testing the wear on a pin-on-disk machine. After machining, the flat surface of the cylindrical test specimen was subjected to a precision grinding process to achieve surface roughness below 0.8 µm arithmetic average.

Fig. 3 (c) Samples

2.2.3. Heat Treatment of Nanocomposites

Heat treatment was done to eliminate the effect of residual stresses due to the machining on the CNC lathe. The test specimens were subjected to a heat treatment process at 400°C for 150 minutes, then cooled at ambient temperature.

2.2.4. Hardness Test

The hardness of nanocomposites is an important parameter that strongly influences the wear behavior of fabricated MMNCs. To obtain the hardness data, a Brinell hardness tester is used. The test is conducted according to standardized procedures (through ASTM E10-18 for Brinell Hardness of Metallic Materials on a scale of HBW 5/250) which was conducted on the specimen before and after heat treatment.

2.2.5. Wear Test on Pin-on-Disk Apparatus

DUCOM's pin-on-disk tribometer was used to obtain friction and wear data (Figure 4).

Fig. 4 Pin on disk apparatus

The apparatus consists of a variable speed motor 200-2000rpm and a spindle, which is connected to a rotating 8mm thick En31 materialled disc hardened to 60HRc of diameter 165mm with the surface roughness ground to 1.6 Ra. A lever arm holds the sample maximum of up to 10mm diameter to be tested at one end and an arrangement for applying load at another end. Friction and wear measuring sensors mounted on the apparatus give instantaneous friction and wear values. These sensor data are recorded and stored in computer memory by using WINDUCOM 2010 software. The wear tests were conducted as per ASTM G 99-17 standard. Samples prepared in the previous steps are subjected to different loading and speed conditions, and the final wear in micrometres with an average value of friction is noted at room temperature. The track diameter was fixed at 40 mm for all tests. A suitable combination of load and speed is selected based on the Taguchi orthogonal array. The test cycle time was set at five minutes for each sample.

2.2.6. Taguchi Design of Experiments

Usually, we conduct experiments to investigate the effects of our expected parameters on the performance of a component. Sometimes, it is also required to find the right combination of input parameters and their level which will provide an optimum response. Design of Experiments (DOE) or experimental design guides us to achieve the above-mentioned targets [20]. The DOE process mainly consists of selecting the expected parameters that can influence the performance and then hypothesizing the selected parameters will not affect the response variable. This type of hypothesis is known as the null hypothesis. The next step consists of the selection of a suitable statistical analysis technique to assess the null hypothesis. After the selection of statistical techniques, different tests are performed, and the obtained data are analysed to either accept or reject the null hypothesis [21].

Taguchi DOE incorporates all the above-mentioned requirements of a general experimental design. It is one of the most commonly used experimental techniques in the engineering field. It is a blend of statistical and engineering techniques that tends to obtain maximum information with a minimum number of tests. It also reduces the cost of experimentation.

The main steps of the Taguchi design of the experiment, as shown in Figure 5, are listed below.

Selection of Factors

It is the first step in Taguchi DOE in which suitable performance parameters, which influence the response variables, are selected by different methods, including brainstorming, Ishikawa diagram and the process of failure analysis. Based on the literature survey and brainstorming process, aluminium alloy, reinforcement weight fraction, load, and speed are considered a factor that influences the response variables.

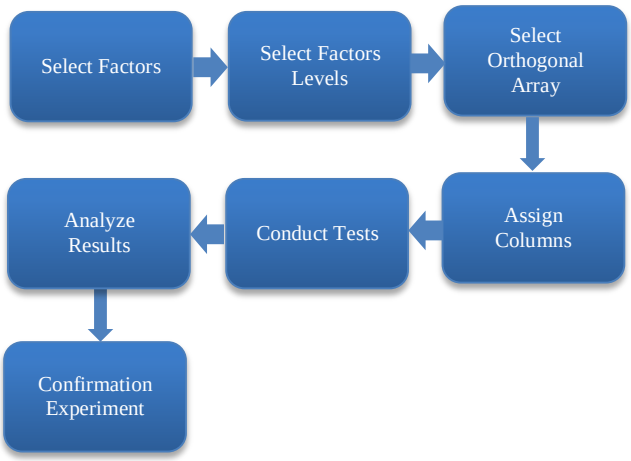

Fig. 5 Steps in taguchi design of experiment

Selection of Factor Levels

In this step, factors are assigned with the specific levels. In the initial Taguchi DOE, the maximum number of factors are incorporated with a minimum number of levels. Mainly, two or three levels of factors are recommended. After consulting with different design engineers, levels of each factor are selected. The alloy factor is set at three different alloy compositions, which include Al 6063, Al6082 and Al 7075. Reinforcement is set at 6, 9. and 12 wt.% of ZrB_2. The load was set as 30N, 40N, and 50N and speeds as 140, 150, and 160 rpm.

Selection of Orthogonal Array

It is a hassle-free method in the Taguchi DOE, where a suitable orthogonal array is chosen based on previously selected factors and their levels. The orthogonal array is a matrix in which each column is subjected to an identical number of conditions. Since there are three factors of three levels each, the L_{27} orthogonal array is selected.

Assign Factors to Columns

Factors are assigned to different columns of the orthogonal array. Alloy and reinforcement are assigned to the first and second columns of the orthogonal array, while load and speed are assigned to the third and fourth columns.

Test Conduction

In this step, by setting the values of factors at the specified level, tests are conducted randomly according to the orthogonal array. Response variables are also noted for further analysis. Tests are conducted on a pin-on-disk machine with different combinations of parameters, and friction and wear values are noted for each run.

Analyse the Obtained Data

Response variables are analysed to find the effects of each factor and their levels. To quantify the effect of each variable, Taguchi recommended using the signal to noise ratio. Then signal, to noise ratio is defined for the following three cases of response variables [22].

- Nominal is the best
- Smaller the better
- Larger the better

Based on the calculated S/N ratio, major influencing factors and the levels at which optimum response is achieved are identified.

Conduction of Confirmation Experiments

To verify the result, a confirmation test was conducted based on the optimum combination of parameters.

2.2.7. Material Characterization Techniques

These are a set of different processes which are crucial for any research work involving material science. These processes are mainly used to determine the physical, mechanical, microstructural, and chemical properties of materials. Microscopy technique, i.e., SEM is used in the process to obtain the required data. SEM is used to obtain high-resolution images of the surface, which are obtained after testing samples on the pin on a disk machine. The SEM images are further used to investigate the dominating wear mechanisms in different nanocomposites. EDX analysis was also conducted on the worn surface to determine its composition.

3. Results and Discussion

3.1. The Effect on Hardness

The hardness data obtained from the Brinell hardness test, which was conducted before and after the heat treatment process, shows different trends for all three aluminium alloys. By comparing the hardness values for each alloy before and after heat treatment, one can say that the hardness value decreases due to the heat treatment process (Figure 6). This decrease in hardness values is more significant in the case of Al 7075 nanocomposites, while Al 6063 nanocomposites showed only a slight change in hardness. Al 6082 nanocomposites showed somewhat intermediate behavior between the above two cases.

If the hardness is compared after heat treatment, it can be concluded that Al 7075 shows the highest hardness, followed by Al 6082 and Al6063 (Figure 7). It can also be concluded that the hardness of Al 6063 increased due to the addition of ZrB_2. The hardness value of Al 7075 first increased and then decreased with an increase in reinforcement weight fraction. Al 6063 shows a decrease in hardness, but there is no significant change in hardness as reinforcement weight fraction increases from 6 to 12 %.

3.2. Taguchi Optimization Process

Taguchi's design of the experiment was adapted to analyse the wear and friction data. L_{27} orthogonal array was selected for the three-factor design with three levels each. To study the effect of each factor, the S/N ratio was calculated based on the minimum of the better criteria. Factors and selected levels are shown in Table 3. Table 4 shows an L_{27} orthogonal array with the friction and wear data.

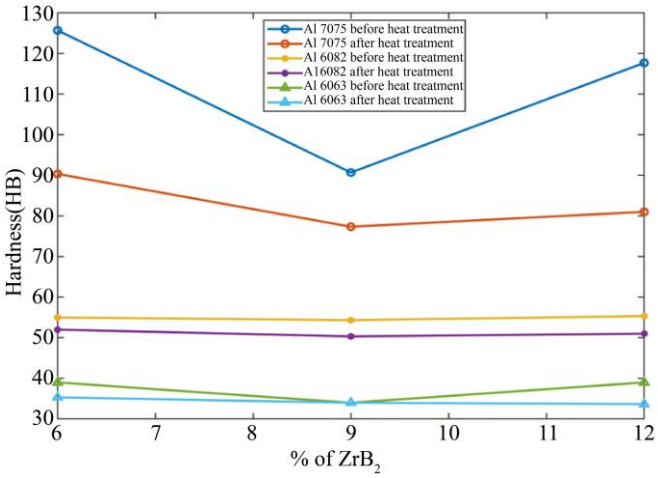

Fig. 6 Variation of hardness of nanocomposites before and after heat treatment

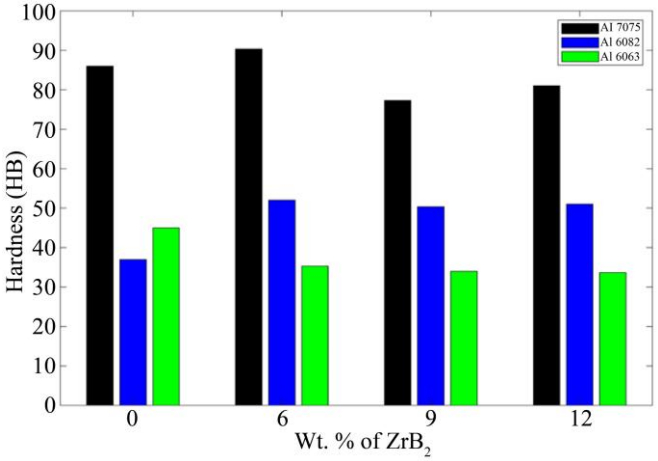

Fig. 7 Variation of hardness of nanocomposites with reinforcement content (after heat treatment process)

Table 3. Selected factors and their levels

Factor	Levels	Values
Alloy	3	6063, 6082, 7075
Reinforcement (%)	3	6, 9, 12
Load (N)	3	30, 40, 50
Speed (rpm)	3	140, 150, 160

3.3. Wear Analysis

Based on the Taguchi statistical analysis, it is concluded that the base alloy composition ranked first has the most significant role in controlling the wear behavior of the nanocomposite. Reinforcing weight fraction also played a major role (which is ranked second after the base alloy composition) in influencing wear behavior. The applied load and speed are also important factors influencing the wear rate, which are ranked third and fourth. Figure 8 shows the S/N ratio variations for the selected factors.

Table 4. L27 orthogonal array with wear and friction data

Alloy	Reinforcement (%)	Load (N)	Speed (rpm)	Wear Rate (mm^3/Nm)	COF
7075	6	30	140	0.055	0.308
7075	6	40	150	0.061	0.320
7075	6	50	160	0.065	0.328
7075	9	30	150	0.054	0.285
7075	9	40	160	0.059	0.325
7075	9	50	140	0.058	0.332
7075	12	30	160	0.045	0.263
7075	12	40	140	0.044	0.269
7075	12	50	150	0.049	0.320
6082	6	40	140	0.071	0.351
6082	6	50	150	0.077	0.364
6082	6	30	160	0.071	0.342
6082	9	40	150	0.064	0.359
6082	9	50	160	0.072	0.360
6082	9	30	140	0.059	0.339
6082	12	40	160	0.061	0.344
6082	12	50	140	0.057	0.358
6082	12	30	150	0.051	0.331
6063	6	50	140	0.095	0.436
6063	6	30	150	0.087	0.423
6063	6	40	160	0.094	0.431
6063	9	50	150	0.092	0.410
6063	9	30	160	0.087	0.397
6063	9	40	140	0.085	0.423
6063	12	50	160	0.084	0.395
6063	12	30	140	0.072	0.384
6063	12	40	150	0.080	0.363

3.3.1. Effect of Alloy Composition on Wear Rate

The composition of base alloys has a significant role in deciding the properties of nanocomposites. The tribological properties of nanocomposites also depend on the properties of the base alloys selected [23, 24]. Figure 8 shows the highest value of the S/N ratio for Al 7075 alloy, followed by Al 6082 and Al 6063. Since there is a steep increase in the S/N ratio for the given alloy composition, one can say that the composition of different aluminium grades strongly influences the wear rate. The minimum value of wear rate is obtained for Al7075 grade which can be correlated with its higher hardness values. Similarly, one can also correlate the wear rates of Al 6082 and Al 6063 with corresponding hardness values.

3.3.2. Effect of Reinforcement on Wear Rate

Like base alloys, the type and weight fraction of nanoparticles also affect the wear rate of nanocomposites. The increase in wear resistance with the addition of ZrB_2 nanoparticles in different matrix metals is also reported in the literature by many researchers [25, 26]. The increase in the S/N ratio is observed with the increase in the weight fraction of reinforcement in the nanocomposite (Figure 8). This increase in the S/N ratio indicates that the wear rate decreases with the increase in reinforcement weight fraction.

A large increase in the S/N ratio is observed by increasing the ZrB_2 weight fraction from 9% to 12% when compared with the increase in the S/N ratio when increasing from 6% to 9%. Thus, it is concluded that a significant increase in wear can be achieved by increasing the ZrB_2 nanoparticle weight fraction from 9% to 12% instead of increasing it from 6% to 9%.

3.3.3. Effect of Load on Wear Rate

Mainly the wear rate increases with the increase in load. Again, as per the literature, it is observed that the tribological behaviour of MMNCs showed an increase in the wear rate. [27]. A similar conclusion can be drawn by observing the S/N ratio plot for the load. Figure 8 shows a steady decrease in the S/N ratio with the increase in the load, which also indicates the increase in wear rate with the load.

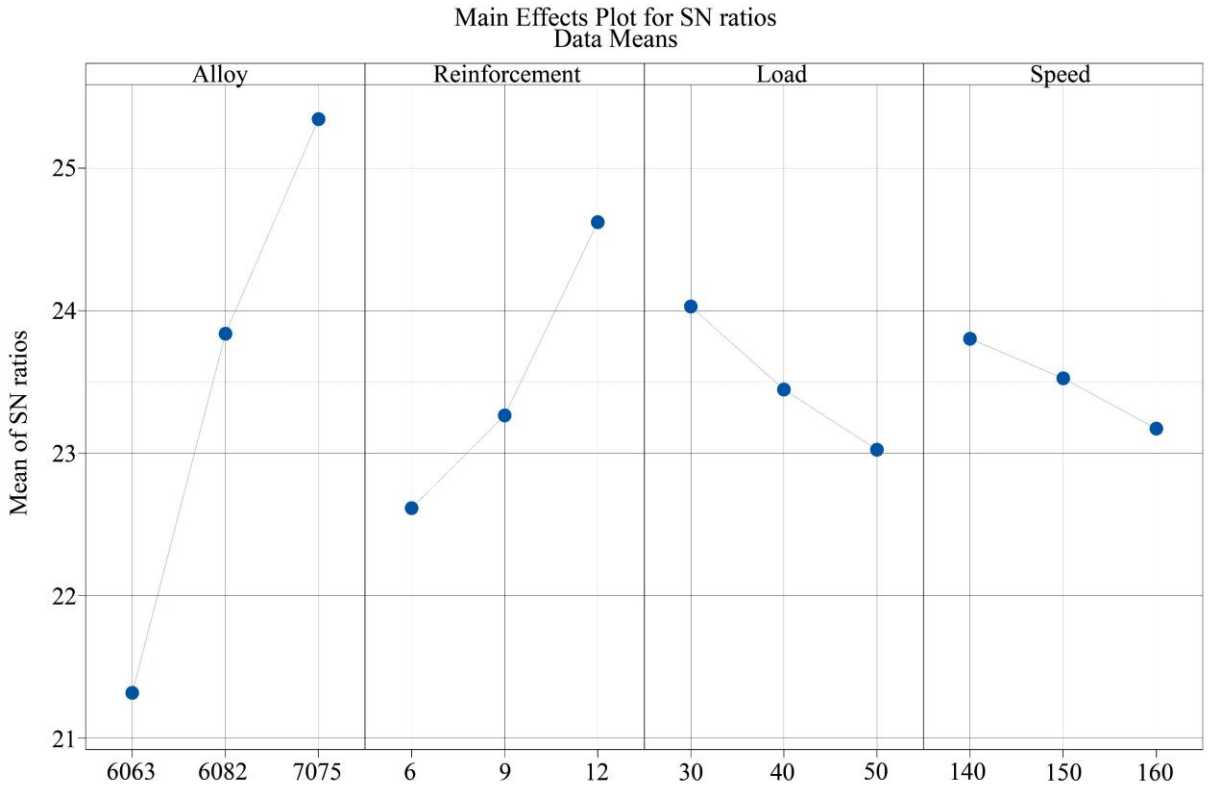

Fig. 8 S/N ratio plot for wear

Table 5. Confirmation experiment for wear

Factors	Levels	Wear (mm^3/Nm)		Error (%)
Alloy	Al 7075	Predicted	Experimental	4.40
Reinforcement (% ZrB_2)	12	0.039227	0.0375	
Load (N)	30			
Speed (rpm)	140			

3.3.4. Effect of Sliding Speed on Wear Rate

The wear rate of nanocomposites increases with the increase in speed for a fixed time interval [28]. Figure 8 shows a decrease in the S/N ratio with the increase in speed, which also indicates an increase in the wear rate with the increase in the sliding speed. This increase in wear rate may be attributed to the increase in the sliding distance with the increase in the speed as the cycle time for testing was fixed.

From the above analysis, it is concluded that the combination of Al 7075 as a base alloy with 12 wt.% ZrB_2 as reinforcement, along with load and speed at 30 N and 140 rpm, gives the optimum wear resistance. Since this combination of input parameters is not available in the orthogonal array, a confirmation test was conducted. The predicted value and actual value of the wear rate are compared (Table 5), which shows a small error of 4.40%.

3.4. Analysis of Coefficient of Friction (COF)

Friction data collected from testing on pin-on-disk tribometer are analysed using the Taguchi statistical technique. Similar to the wear test results, alloy and reinforcement are the most significant factors which are ranked first and second. The applied load also strongly affects the COF value, which is ranked third in the Taguchi analysis. The sliding speed has minimal effect on COF, which is ranked fourth. Figure 9 shows the S/N ratio variation for the factors considered in Taguchi analysis.

3.4.1. Effect of Alloy Composition

The Coefficient of Friction (COF) is a system property that depends on variables like the types of materials in contact with each other, their compositions, hardness values, and temperature [29]. Figure 9 presents the effect of the alloy composition on COF, which shows the increase in the S/N ratio as the alloy composition changes from Al 6063 to Al 6082 and from Al 6082 to Al 7075. The difference in the S/N ratio is larger, which shows that alloy composition strongly influences wear rate. Since the S/N ratio is highest for Al 7075, it has the lowest COF, followed by Al 6082, which has lower COF values than Al 6063.

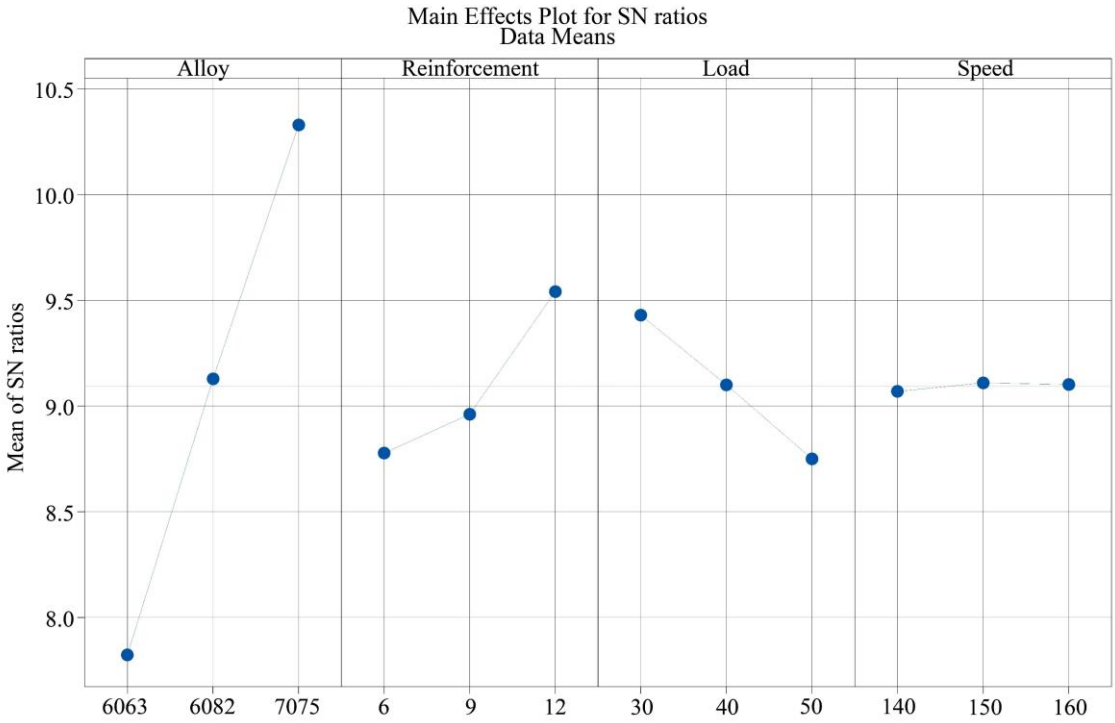

Fig. 9 S/N ratio plot for COF

Table 6. Confirmation experiment for COF

Factors	Levels	COF		Error (%)
Alloy	Al 7075	Predicted	Experimental	5.36
Reinforcement (% ZrB_2)	12	0.2779	0.263	
Load (N)	30			
Speed (rpm)	160			

3.4.2. Effect of Reinforcement

Most of the research has reported a decrease in COF due to the application of nanoparticles in the different matrix metals [30, 31]. The effect of the reinforcement factor on COF shows a similar trend as in the case of wear rate. When the reinforcement content increased from 6 to 12 wt.%, the values of the S/N ratio correspondingly increased. This increase in the S/N ratio is greater when the ZrB_2 nanoparticle weight fraction increases from 9 to 12% compared to increasing from 6 to 9%. Thus, it is concluded that lower COF can be obtained at a higher weight fraction of reinforcement.

3.4.3. Effect of Load

The Coefficient of Friction (COF) increases with load for different material pairs [32]. A steady decrease in the S/N ratio with the increase in the load is observed in Figure 9. Thus, it is concluded that lower COF was obtained with reduced load.

3.4.4. Effect of Sliding Velocity

The laws of friction state that COF is independent of the sliding velocity [26, 23]. This can also be verified by observing Figure 9, which shows minor variations with the increase in speed. However, the highest value of the S/N ratio is observed at a speed of 160 rpm.

Thus, from the above analysis, it is concluded that a combination of Al 7075 as a base alloy with 12 wt.% ZrB_2 nano reinforcement along with the load at 30 N and sliding speed at 160 rpm gives an optimum value of COF. Since this combination of factor levels is already present in an orthogonal array, a separate confirmation experiment is not required in this case. A comparison between the predicted value and the experimental value of the coefficient of friction (Table 6) shows a small error of 5.34%.

3.5. Analysis of Variance

ANOVA is a statistical technique that is mostly used in the research field to determine if the difference in performance is due to natural variations because of unassignable causes or due to changes in the controllable factor levels. The ANOVA test was performed on S/N data of wear rate and coefficient of friction with alloys, reinforcement, load and speed. The confidence level was set at 95%, and error variance and factor variance were then calculated. The ratio of factor variance to error variance, called F-ratio, is then calculated. This calculated F-ratio, along with the factor degree of freedom and error degree of freedom, is used to calculate the p-value. For a 95% confidence level, if the p-value is less than 0.05, then the factor is considered as significant.

Table 7. ANOVA table for wear

Source	DF	Seq SS	Adj SS	Adj MS	F	P
Alloy	2	74.523	74.523	37.2613	389.33	0.000
Reinforcement	2	18.878	18.878	9.4392	98.63	0.000
Load	2	4.577	4.577	2.2883	23.91	0.000
Speed	2	1.796	1.796	0.8982	9.39	0.002
Residual Error	18	1.723	1.723	0.0957		
Total	26	101.497				

Table 8. ANOVA table for COF

Source	DF	Seq SS	Adj SS	Adj MS	F	P
Alloy	2	28.2594	28.2594	14.1297	95.88	0.000
Reinforcement	2	2.8603	2.8603	1.4301	9.70	0.001
Load	2	2.0739	2.0739	1.0370	7.04	0.006
Speed	2	0.0082	0.0082	0.0041	0.03	0.973
Residual Error	18	2.6527	2.6527	0.1474		
Total	26	35.8545				

The results of the ANOVA test for wear rate in Table 7 are summarized, which shows all the factors considered for testing, including alloys, reinforcement, load, and speed, are significant. Similarly, ANOVA test results for the coefficient of friction in Table 8, alloys, reinforcement and load are significant factors since their p-value is lower than 0.05. Sliding speed in the case of COF is not a significant factor because of a greater p-value than 0.05. Residual plots for wear and COF are represented in Figures 10 and 11. The histogram in both cases of wear and COF suggests the normal distribution of residuals. The normal distribution of residuals can also be observed from normal probability for both COF and wear.

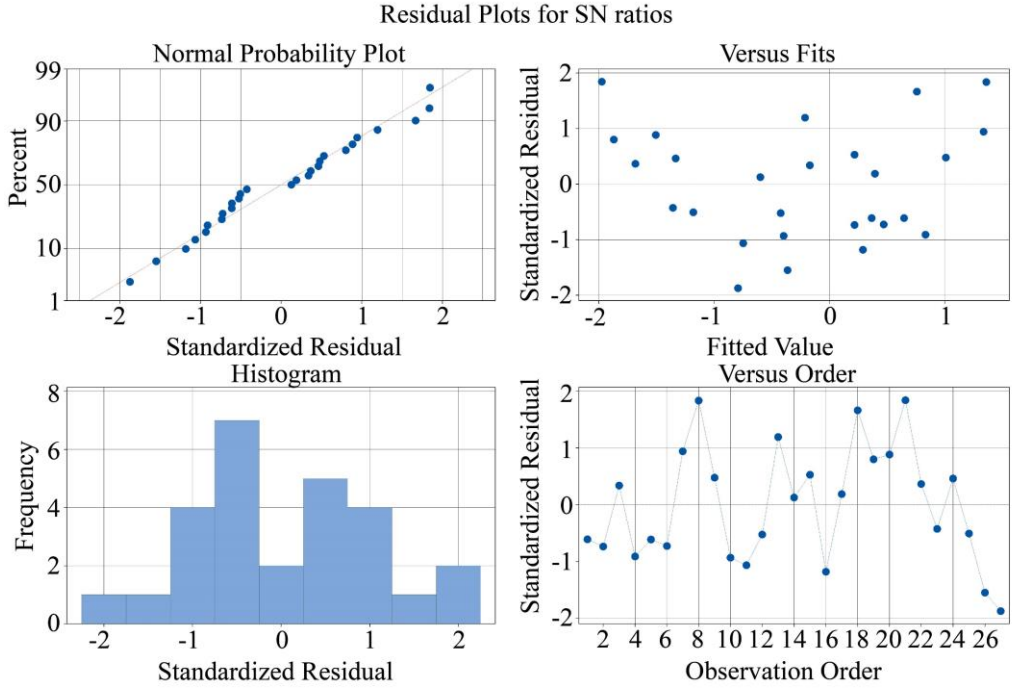

Fig. 10 Residual plots for wear

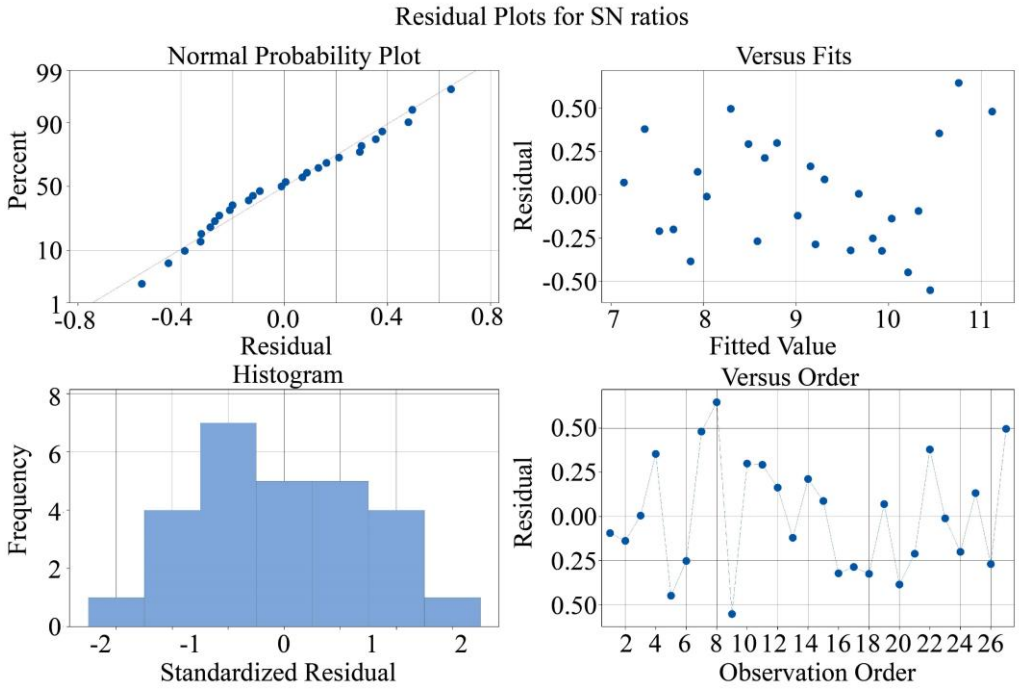

Fig. 11 Residual plots for COF

3.6. SEM Analysis of Worn Surface

To analyse the effect of reinforcement on aluminium alloys, SEM was performed on the worn surface at room temperature by keeping the other parameters like the load and speed constant for all the samples. Figures 12-14 show SEM images of Al 6063, Al6082, and Al7075 with reinforcement content varying from 6 to 12%. These SEM images are analysed to find the dominating wear mechanisms in each alloy.

3.6.1. Al 6063 Nanocomposites

Significant plastic deformation and ploughing of the surface were observed for Al 6063 nanocomposites. The decrease in groove size is observed with the increase in the weight fraction of ZrB_2 from 6% to 12%, which are marked by green arrows. This may be due to the higher ductility of base alloy and lower hardness values of Al 6063 nanocomposites. The presence of grooves, along with the flow of the materials, indicates the presence of an adhesive wear mechanism in the nanocomposites.

Figure 12 shows higher surface damage for Al 6063-12% ZrB_2 nanocomposite. This may be due to the combined effect of adhesive and abrasive wear mechanisms. The effect of the abrasive wear mechanism dominates for nanocomposites with higher reinforcement content. As the effects of the abrasive wear mechanism start dominating the adhesive wear mechanism, wear debris on the surface of nanocomposites increases. The red circles mark the wear debris. Surface cracks and flake-like debris increase with the increase in reinforcement content, which is marked by yellow squares. This increase in the surface cracks and flakes-like debris indicates the presence of a delamination wear mechanism.

3.6.2. Al 6082 Nanocomposites

Similar to Al 6063 nanocomposites, the width of the grooves and the plastic flow of the material in the case of Al 6082 nanocomposites decreased with the reinforcement weight fraction (Figure 13), which indicates the decrease in the effects of adhesive wear mechanism with the increased in reinforcing weight fraction. The overall damage to the surface was reduced as the reinforcement weight fraction increased from 6% to 12% ZrB_2. The overall content of wear debris and flake-like debris also decreased with the increase in reinforcement content. This reduction in wear debris and subsurface cracks shows the declining surface damaging effects of abrasive and delamination wear mechanisms. Thus, it is concluded that the addition of nanoparticles in Al 6082 alloy enhances its wear properties.

3.6.3. Al 7075 Nanocomposites

SEM images of Al 7075 nanocomposites showed a reduction in surface damage with the increase in the weight fraction of nanoreinforcement (Figure 14). The size of the grooves, along with the plastic flow of the material, decreases with the increase in reinforcement weight fraction, which indicates a decrease in the adhesive wear mechanism. Wear debris and surface cracks are also decreased with the increase in ZrB_2 reinforcement weight fraction. This decrease indicates a reduction in the surface damaging effects of the abrasive wear mechanism and delamination wear mechanism.

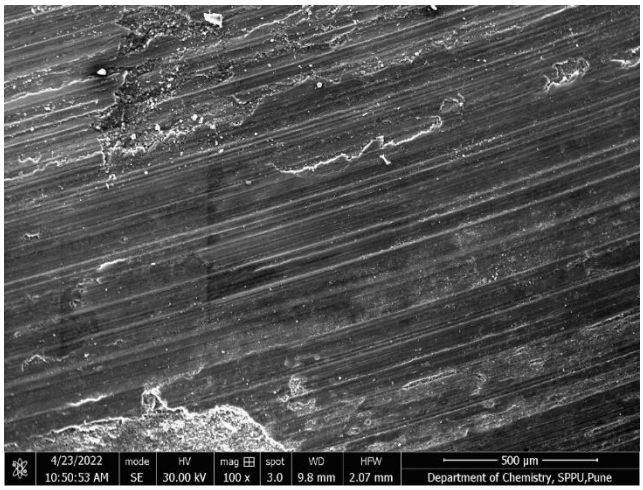

(a)

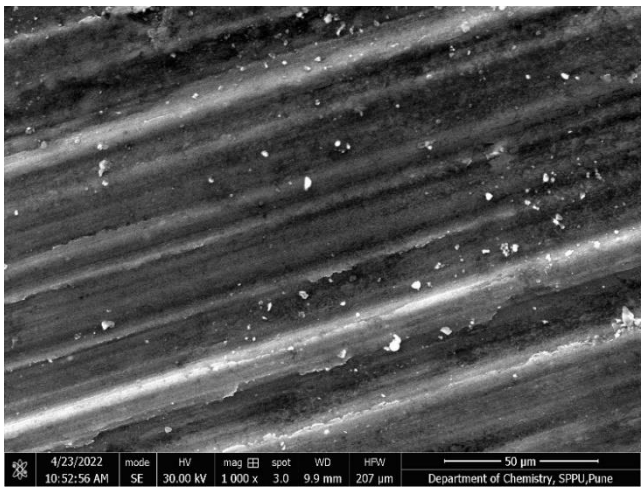

(b)

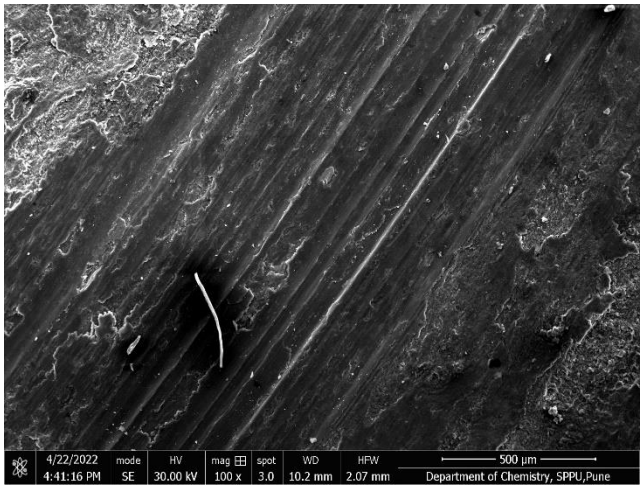

(c)

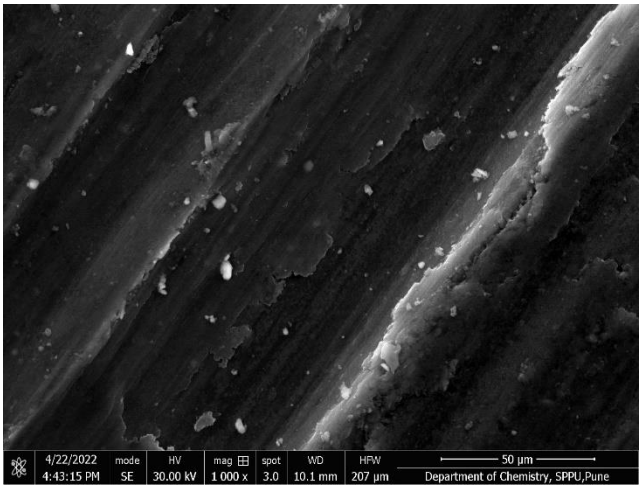

(d)

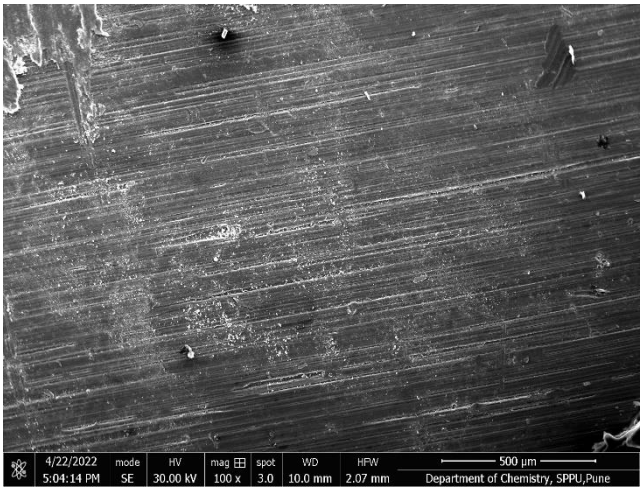

(e)

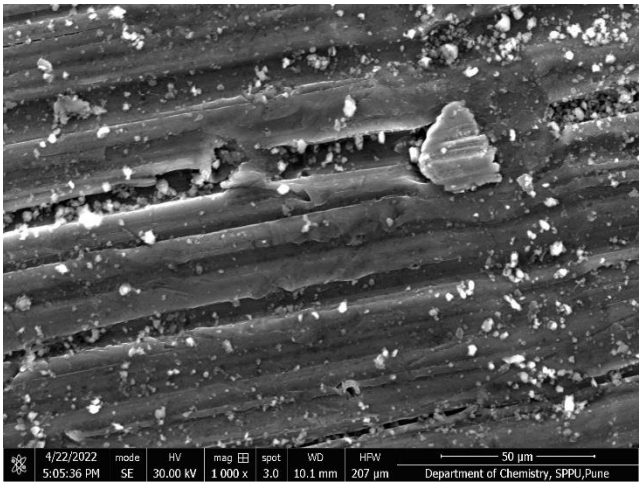

(f)

Fig. 12 SEM images of Al 6063 nanocomposites (a, b) with 6% ZrB_2, (c, d) with 9% ZrB_2, and (e, f) 12% ZrB_2.

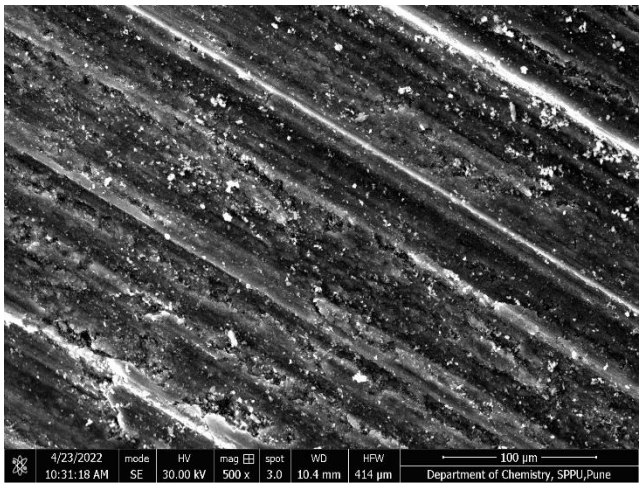

(a)

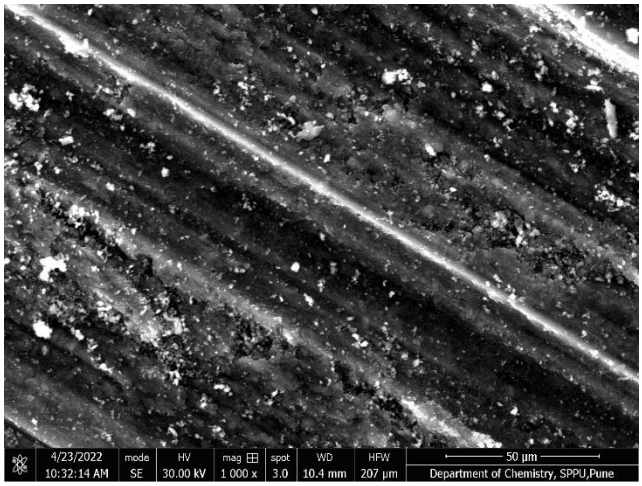

(b)

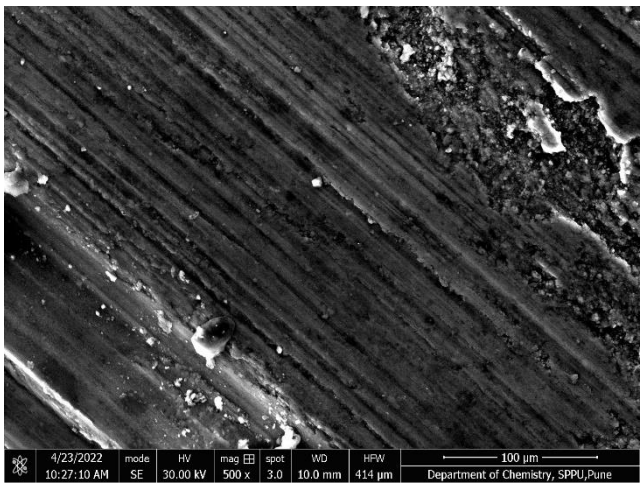

(c)

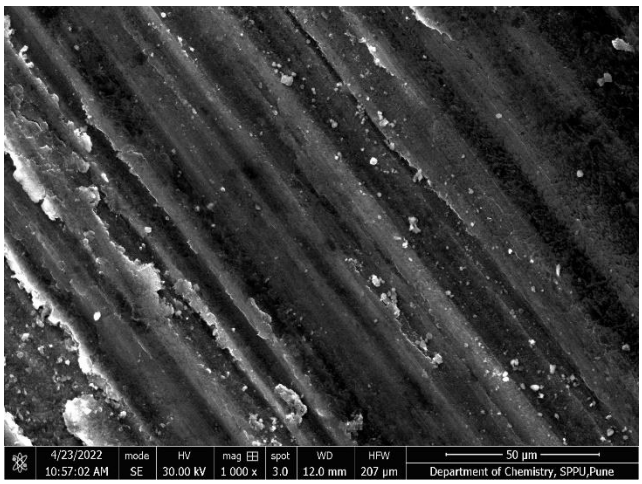

(d)

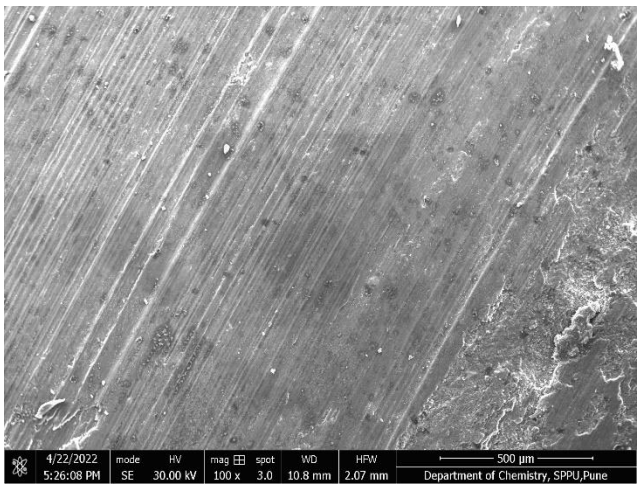

(e)

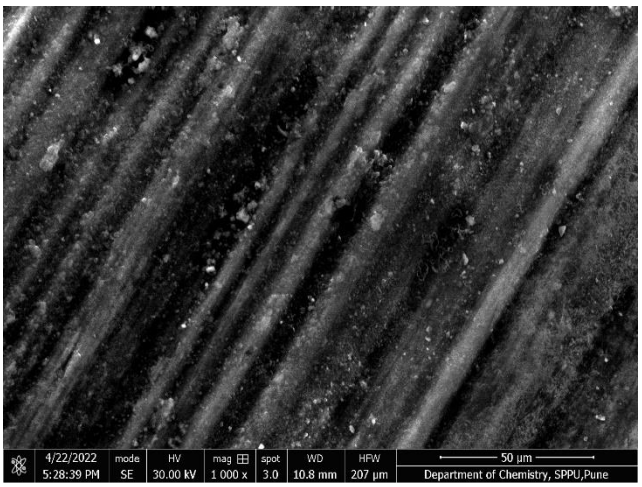

(f)

Fig. 13 SEM images of Al 6082 nanocomposites (a, b) with 6% ZrB_2, (c, d) with 9% ZrB_2, and (e, f) 12% ZrB_2.

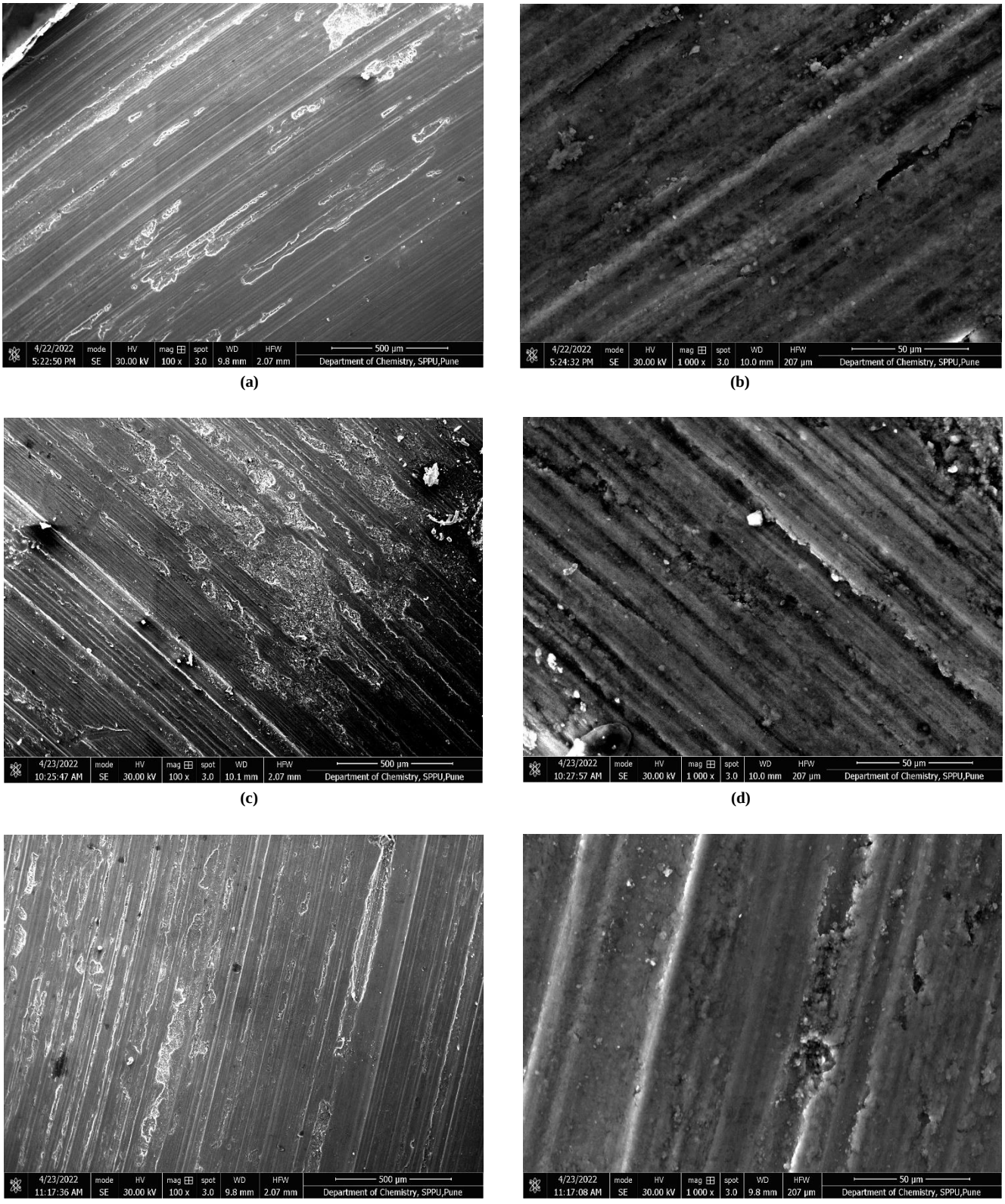

Fig. 14 SEM images of Al 7075 nanocomposites (a, b) with 6% ZrB_2, (c, d) with 9% ZrB_2, and (e, f) 12% ZrB_2.

3.7. EDX Analysis

EDX was performed to know the composition of various constituents of the worn surface. Al 6063 with 12% ZrB2 was selected for EDX analysis. Figure 15 shows the composition of the surface. The formation of the oxide layer is confirmed by the EDX analysis, which shows a peak corresponding to oxygen (O) (Figure 15). This oxide layer is formed due to the heat that is generated from friction between the disk and pin surface.

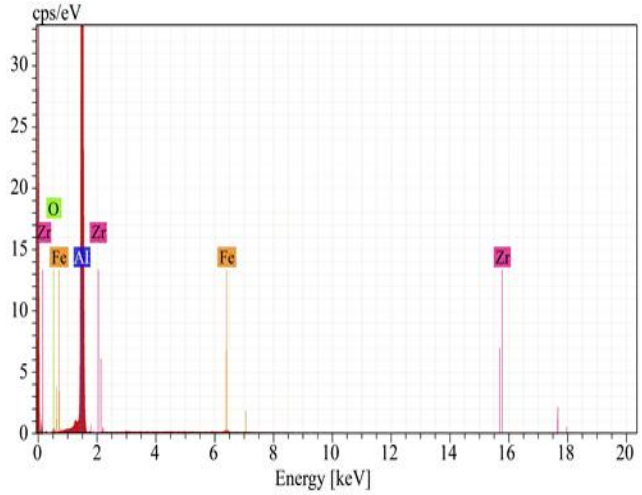

Fig. 15 EDX of Al 6063-12% ZrB2 nanocomposite

The formation of the oxide layer helps to reduce the wear rate of the nanocomposite. A transfer of some material from the disk to the pin surface was observed from the peak corresponding to iron (Fe). Some traces of Zirconium (Zr) were also detected due to the presence of reinforcement in the aluminium matrix.

4. Conclusion

The main aim of this work is to obtain an optimum combination of alloys, reinforcement, load and speed from their selected levels. Taguchi's design of the experiment, along with its statistical technique, is adapted to find the optimum combination of factor levels. The effect of heat treatment on the hardness of fabricated nanocomposite is also investigated.

The conclusions drawn from the analysis of the worn surfaces to obtain the probable wear mechanism are listed below.

1. The heat treatment process affects the hardness of the nanocomposites. The effect of heat treatment was most significant on Al 7075 nanocomposites, followed by Al 6082 and Al 6063.
2. From the Taguchi analysis, it is concluded that Al 7075 showed better wear resistance, followed by Al 6082 and Al 6063. The increase in ZrB_2 weight fraction increases wear resistance for all the selected aluminium alloys.
3. ANOVA test results for wear rate showed alloy and reinforcement weight fraction as the most significant contributing factor. Load and speed are also identified as significant factors.
4. Aluminium 7075 alloy reinforced with 12% ZrB_2 along with load and speed values at 30 N and 140 rpm gives the optimum wear rate.
5. Taguchi analysis also showed the lowest COF for Al 7075 nanocomposites, followed by Al 6082, which has a lower COF than Al 6063.
6. Similar to the wear rate, the COF of nanocomposites also decreases with the increase in the ZrB_2 nanoparticle weight fraction.
7. Alloy grade, reinforcement weight fraction and applied load are identified as significant factors influencing COF from the ANOVA analysis.
8. Aluminium 7075 alloy reinforced with 12% ZrB_2 along with load and speed values at 30 N and 160 rpm gives the optimum COF.
9. From the SEM analysis of the worn surface, it is observed that the adhesive wear mechanism dominated for Al 6063 nanocomposites. Al 6082 and Al 7075 nanocomposites show abrasion and delamination as dominating wear mechanisms, with adhesive wear having a significant role in nanocomposites with lower reinforcement weight fraction.
10. EDX analysis of Al 6063-12% ZrB_2 confirmed the presence of the oxide layer on the worn surface which helps to reduce the wear rate.

References

[1] Erik Tempelman, *Chapter 18 - Lightweight Materials, Lightweight Design*?, Materials Experience: Fundamentals of Materials and Design, pp. 247-258, 2014. [CrossRef] [Google Scholar] [Publisher Link]

[2] A. Erman Tekkaya, and Junying Min, "Special Issue on Automotive Lightweight," *Automotive Innovation*, vol. 3, pp. 193-194, 2020. [CrossRef] [Google Scholar] [Publisher Link]

[3] Horst E. Friedrich, "Lightweight Engineering and Material Innovations in Automotive Engineering," *ATZ Worldwide*, vol. 104, pp. 24-27, 2002. [CrossRef] [Google Scholar] [Publisher Link]

[4] L. Zhu, N. Li, and P.R.N. Childs, "Light-Weighting in Aerospace Component and System Design," *Propulsion and Power Research*, vol. 7, no. 2, pp. 103-119, 2018. [CrossRef] [Google Scholar] [Publisher Link]

[5] Jihye An et al., "A Study on the Wear Characteristics of Al7075 with Changes in Surface Roughness and Ti Thin Film Deposition Time," *Advances in Materials Science and Engineering*, vol. 2020, no. 1, pp. 1-9, 2020. [CrossRef] [Google Scholar] [Publisher Link]

[6] L. Feroz Ali et al., "Microstructural and Wear Behaviour of Al 6063–W Nanocomposites Developed Using Friction Stir Processing," *Metals and Materials International*, vol. 27, pp. 5462-5473, 2021. [CrossRef] [Google Scholar] [Publisher Link]

[7] M. Ramachandra et al., "Hardness and Wear Resistance of ZrO_2 Nano Particle Reinforced Al Nanocomposites Produced by Powder Metallurgy," *Procedia Materials Science*, vol. 10, pp. 212-219, 2015. [CrossRef] [Google Scholar] [Publisher Link]

[8] Priyaranjan Samal, Ravi Kumar Mandava, and Pandu R. Vundavilli, "Dry Sliding Wear Behavior of Al 6082 Metal Matrix Composites Reinforced with Red Mud Particles," *SN Applied Sciences*, vol. 2, pp. 1-11, 2020. [CrossRef] [Google Scholar] [Publisher Link]

[9] Huda A. Al-Salihi, Adil Akram Mahmood, and Hussain J. Alalkawi, "Mechanical and Wear Behavior of AA7075 Aluminum Matrix Composites Reinforced by Al_2O_3 Nanoparticles," *Nanocomposites*, vol. 5, no. 3, pp. 67-73, 2019. [CrossRef] [Google Scholar] [Publisher Link]

[10] Krishna Mohan Singh, and Akhilesh Kumar Chauhan, "Fabrication, Characterization, and Impact of Heat Treatment on Sliding Wear Behaviour of Aluminium Metal Matrix Composites Reinforced with B_4C," *Advances in Materials Science Engineering*, vol. 2021, no. 1, pp. 1-9, 2021. [CrossRef] [Google Scholar] [Publisher Link]

[11] J.C. Benedyk, *3 -Aluminum Alloys for Lightweight Automotive Structures*, Materials, Design and Manufacturing for Lightweight Vehicles, Woodhead Publishing Series in Composites Science and Engineering, pp. 79-113, 2010. [CrossRef] [Google Scholar] [Publisher Link]

[12] A.P. Mouritz, *8- Aluminium Alloys for Aircraft Structures*, Introduction to Aerospace Materials, pp. 173-201, 2012. [CrossRef] [Google Scholar] [Publisher Link]

[13] Christian Vargel, *Chapter A.4 - Aluminium Alloy Series*, Corrosion of Aluminium, pp. 17-20, 2020. [CrossRef] [Google Scholar] [Publisher Link]

[14] Prantik Mukhopadhyay, "Alloy Designation, Processing, and Use of AA6XXX Series Aluminium Alloys," *International Scholarly Research Notices*, vol. 2012, no. 1, pp. 1-15, 2012. [CrossRef] [Google Scholar] [Publisher Link]

[15] William G. Fahrenholtz et al., "Refractory Diborides of Zirconium and Hafnium," *Journal of the American Ceramic Society*, vol. 90, no. 5, pp. 1347-1364, 2007. [CrossRef] [Google Scholar] [Publisher Link]

[16] Carmen M. Cepeda-Jiménez, and María T. Pérez-Prado, "4.12 Processing of Nanoparticulate Metal Matrix Composites," *Reference Module in Materials Science and Materials Engineering, Comprehensive Composite Materials II*, vol. 4, pp. 313-330, 2018. [CrossRef] [Google Scholar] [Publisher Link]

[17] Mehrdad Shayan, Beitallah Eghbali, and Behzad Niroumand, "Fabrication of AA2024–TiO_2 Nanocomposites through Stir Casting Process," *Transactions of Nonferrous Metals Society of China*, vol. 30, no. 11, pp. 2891-2903, 2020. [CrossRef] [Google Scholar] [Publisher Link]

[18] Hamid Reza Ezatpour et al., "Investigation of Microstructure and Mechanical Properties of Al6061-Nanocomposite Fabricated by Stir Casting," *Materials & Design*, vol. 55, pp. 921-928, 2014. [CrossRef] [Google Scholar] [Publisher Link]

[19] S.A. Sajjadi, H.R. Ezatpour, and H. Beygi, "Microstructure and Mechanical Properties of Al–Al_2O_3 Micro and Nano Composites Fabricated by Stir Casting," *Materials Science and Engineering: A*, vol. 528, no. 29-30, pp. 8765-8771, 2011. [CrossRef] [Google Scholar] [Publisher Link]

[20] Mehdi Mahmoudian et al., "Optimization of Mechanical Properties of in Situ Polymerized Poly (Methyl Methacrylate)/Alumina Nanoparticles Nanocomposites Using Taguchi Approach," *Polymer Bulletin*, vol. 77, pp. 2837-2854, 2020. [CrossRef] [Google Scholar] [Publisher Link]

[21] Joseph Berk, and Susan Berk, *Chapter 11 - ANOVA, Taguchi, and Other Design of Experiments Techniques: Finding Needles in Haystack*, Quality Management for the Technology Sector, pp. 106-123, 2000. [CrossRef] [Google Scholar] [Publisher Link]

[22] J.A. Ghani , I.A. Choudhury, and H.H. Hassan, "Application of Taguchi Method in the Optimization of End Milling Parameters," *Journal of Materials Processing Technology*, vol. 145, no. 1, pp. 84-92, 2004. [CrossRef] [Google Scholar] [Publisher Link]

[23] A. Prasad Reddy, P. Vamsi Krishna, and R.N. Rao, "Tribological Behaviour of Al6061–2SiC-xGr Hybrid Metal Matrix Nanocomposites Fabricated through Ultrasonically Assisted Stir Casting Technique," *Silicon*, vol. 11, pp. 2853-2871, 2019. [CrossRef] [Google Scholar] [Publisher Link]

[24] B. Selvam et al., "Dry Sliding Wear Behaviour of Zinc Oxide Reinforced Magnesium Matrix Nanocomposites," *Materials & Design*, vol. 58, pp. 475-481, 2014. [CrossRef] [Google Scholar] [Publisher Link]

[25] R. Harichandran, and N. Selvakumar, "Effect of Nano/Micro B_4C Particles on the Mechanical Properties of Aluminium Metal Matrix Composites Fabricated by Ultrasonic Cavitation-Assisted Solidification Process," *Archives of Civil and Mechanical Engineering*, vol. 16, pp. 147-158, 2016. [CrossRef] [Google Scholar] [Publisher Link]

[26] Alireza Abdollahi, Ali Alizadeh, and Hamid Reza Baharvandi, "Dry Sliding Tribological Behavior and Mechanical Properties of Al2024–5 wt.%B4C Nanocomposite Produced by Mechanical Milling and Hot Extrusion," *Materials & Design*, vol. 55, pp. 471-481, 2014. [CrossRef] [Google Scholar] [Publisher Link]

[27] Meysam Tabandeh-Khorshid et al., "Tribological Performance of Self-Lubricating Aluminum Matrix Nanocomposites: Role of Graphene Nanoplatelets," *International Journal of Engineering Science and Technology*, vol. 19, no. 1, pp. 463-469, 2016. [CrossRef] [Google Scholar] [Publisher Link]

[28] D. Jeyasimman et al., "The Effects of Various Reinforcements on Dry Sliding Wear Behaviour of AA 6061 Nanocomposites," *Materials & Design*, vol. 64, pp. 783-793, 2014. [CrossRef] [Google Scholar] [Publisher Link]

[29] A.E. Jiménez, and M.D. Bermúdez, *2 - Friction and Wear*, Tribology for Engineers, A Practical Guide, pp. 33-63, 2011. [CrossRef] [Google Scholar] [Publisher Link]

[30] Shubhajit Das et al., "Fabrication and Tribological Study of AA6061 Hybrid Metal Matrix Composites Reinforced with SiC/B_4C Nanoparticles," *Industrial Lubrication and Tribology*, vol. 71, no. 1, pp. 83-93, 2019. [CrossRef] [Google Scholar] [Publisher Link]

[31] Veeravalli Ramakoteswara Rao, Nallu Ramanaiah, and Mohammed Moulana Mohiuddin Sarcar, "Mechanical and Tribological Properties of AA7075–TiC Metal Matrix Composites under Heat Treated (T_6) and Cast Conditions," *Journal of Materials Research and Technology*, vol. 5, no. 4, pp. 377-383, 2016. [CrossRef] [Google Scholar] [Publisher Link]

[32] Suswagata Poria, Prasanta Sahoo, and Goutam Sutradhar, "Tribological Characterization of Stir-cast Aluminium-TiB_2 Metal Matrix Composites," *Silicon*, vol. 8, pp. 591-599, 2016. [CrossRef] [Google Scholar] [Publisher Link]